NASA DEVELOP National Program
Massachusetts – Boston

Summer 2021

Cincinnati & Covington Urban Development II

Assessing Flooding and Landslide Susceptibility Along the Ohio-Kentucky Border

DEVELOP Technical Report

Final – August 12th, 2021

Paxton LaJoie (Project Lead)
Edward Cronin
John Perrotti
Erin Shives
Sophie Webster

Advisors:
Dr. Cedric Fichot, Boston University (Science Advisor)
Dr. Kenton Ross, NASA Langley Research Center (Science Advisor)
Dr. Matt Crawford, Kentucky Geological Survey (Science Advisor)

Previous Contributors:
Olivia Cronin-Golomb
Samuel Feibel
Katrina Rokosz

1. Abstract

Landslides and flooding are reoccurring environmental hazards that lead to health risks and economic burdens in the urban areas of Cincinnati, Ohio and Covington, Kentucky. These communities share underlying natural and artificial conditions that make them vulnerable to these hazards, including excessive precipitation, weak lithology, high impervious surface levels, and steep slopes. Despite the human and economic risks associated with these environmental hazards, the areas of highest vulnerability within the region remain unknown. NASA DEVELOP partnered with Groundwork USA and Groundwork Ohio River Valley (ORV) to assess the region's susceptibility to landslides and flooding. The team utilized NASA Earth observations, including the Landsat 8 Operational Land Imager (OLI), Landsat 8 Thermal Infrared Sensor (TIRS), and Global Precipitation Measurement (GPM) Integrated Multi-satellitE Retrieval for GPM (IMERG), alongside ancillary datasets to map landslide susceptibility and exposure throughout the study area. The resulting landslide susceptibility and exposure maps highlight the neighborhoods around Avondale and Fairmount as areas of particularly high landslide exposure. The team also used ancillary data to map surface runoff and runoff retention using the Natural Capital Project's Integrated Valuation of Ecosystem Services and Tradeoffs (InVEST) Urban Flood Risk Mitigation Model and used those results to identify pluvial flood vulnerability within the region. The InVEST outputs demonstrate that Downtown Cincinnati and the Queensgate neighborhood retain the least amount of rainfall. This research provides partners with a more complete hazard analysis of the greater Cincinnati area while also producing refined methodologies to enhance future flood and landslide vulnerability mapping throughout Groundwork USA's nationwide network of communities.

Key Terms

landslide exposure, InVEST Urban Flood Risk Mitigation Model, runoff retention, precipitation

2. Introduction

2.1 Background Information

Cincinnati, Ohio and Covington, Kentucky are neighboring cities separated by the Ohio River. The region is notably vulnerable to landslides and flooding events, exacerbated by its underlying geology, regular rainfall, and pervasive urban development. These environmental hazards pose a threat to community safety and have required millions of dollars in repairs from local government (Validity and Effectiveness of Landslide Susceptibility Maps, 2004).

Landslides occur when earth is destabilized and gravity overcomes the friction holding the materials intact (Mardon, 2020). They are caused by numerous natural factors, including geology, steep slopes, heavy rainfall, and flaggy soil (Sarkar & Kanungo, 2004). Southwestern Ohio and Northern Kentucky's weak geology and soil makeup render them especially susceptible to slope failure (Cincinnati Department of Transportation and Engineering, 2019). The region is underpinned by the Kope Formation, a fossiliferous bedrock composed of shale and limestone that erodes over time into layers of loose, weathered rock that are easily saturated and destabilized by water (Hansen, 1995). Anthropogenic factors can also increase landslide likelihood. Woody vegetation loss characteristic of urban development weakens slopes nine-fold, as trees create a stabilizing root matrix and absorb water to stall sliding (Riestenberg & Sovonick-Dunford, 1983). Human disturbances such as excavation, filling, and drainage also beget slope instability (Mardon, 2020).

Flood events are closely linked to landslides and are often prompted by similar factors such as water-logged soils, heavy precipitation, and surface runoff. The Ohio River Valley is notorious for flooding caused by concurrent springtime rainfall and snowmelt that overwhelm soil water capacity and drainage systems (Horton and Jackson, 1913). Urbanization heightens pluvial flood risk with more impervious surfaces, vegetation loss, and insufficient drainage that limit runoff retention (Liu et al., 2020). Such environmental hazards take a substantial economic toll on municipalities. Between 2015 and 2019, Ohio spent nearly $300 million repairing landslide damage, while Kentucky spent $85 million repairing state roads alone (Sparling & DeMio, 2019). Historically, Cincinnati has had one of the highest per capita landslide repairs costs nationwide

(Fleming & Taylor, 1980). Urban flooding can be catastrophic, as buildings can be overrun by stormwater and sewage. In this event, homeowners often bear the costs. As natural and anthropogenic factors collide with rainfall and snowmelt, the Ohio River Valley requires modern susceptibility mapping to indicate high priority areas for mitigation efforts.

Fortunately, the use of spatial data in assessing landslide and flooding susceptibility has improved substantially. With growing utilization of remote sensing imagery, landslide susceptibility maps have been generated on a global scale (Hong, Adler, & Huffman, 2006). Historical landslide inventories are a critical first step for cataloging slope failures and potential causes (Van Westen, Castellanos, & Kuriakose, 2008). Such inventories have become publicly available through efforts by the United States Geological Survey (USGS) and the Kentucky Geological Survey. Previous research has identified many of the aforementioned variables (e.g., lithology, soil type, slope) as factors influencing landslide events (Sarkar & Kanungo, 2004; Mardon, 2020).

This DEVELOP project was the second in a two-term project partnership with Groundwork USA and Groundwork Ohio River Valley (ORV). In spring 2021, the MA – Boston DEVELOP team assessed urban heat vulnerability in the Cincinnati and Covington area. The team used the Integrated Valuation of Ecosystem Services and Tradeoffs (InVEST) Urban Cooling Model to create a heat mitigation index for the region. Additionally, the team mapped daytime and nighttime land surface temperature anomalies for the area. To continue assessing climate threats that impact the region's vulnerable communities, the summer 2021 team mapped landslide and flood vulnerabilities facing the local populations.

2.2 Project Partners & Objectives

Groundwork USA and Groundwork ORV partnered with the summer 2021 MA – Boston DEVELOP team to complete this project. Groundwork USA is a network of nonprofit organizations focused on improving urban spaces to help mitigate environmental and socioeconomic inequalities within marginalized communities. Groundwork ORV is focused on expanding environmental awareness and justice through the communication of spatial data. This work will be used to help integrate new NASA Earth observations into their decision-making processes.

For this project, the team's main objectives were to map landslide susceptibility and exposure, as well as identify pluvial flood vulnerability within the region. Landslide susceptibility describes how likely a landslide is to occur based on geologic conditions. Separately, landslide exposure combines landslide susceptibility with population or critical infrastructure data to reveal which target groups are highly impacted by landslides. To create high-resolution landslide susceptibility and exposure maps for the chosen study period (2004 - 2021), the team used a fuzzy logic model approach in ArcGIS Pro. In addition, the team utilized the InVEST Urban Flood Risk Mitigation Model, a product of Stanford's Natural Capital Project. InVEST is a software suite that models natural resources and their economic impacts. Using this model, the team calculated stormwater runoff retention, runoff values, and potential damage in reference to infrastructure within the study area. For this project, the study area was defined as the city of Cincinnati, including the municipalities of Norwood, St. Bernard, and the village of Elmwood Place, as well as the greater Northern Covington area within I-275 in both Kenton and Campbell Counties (Figure 1).

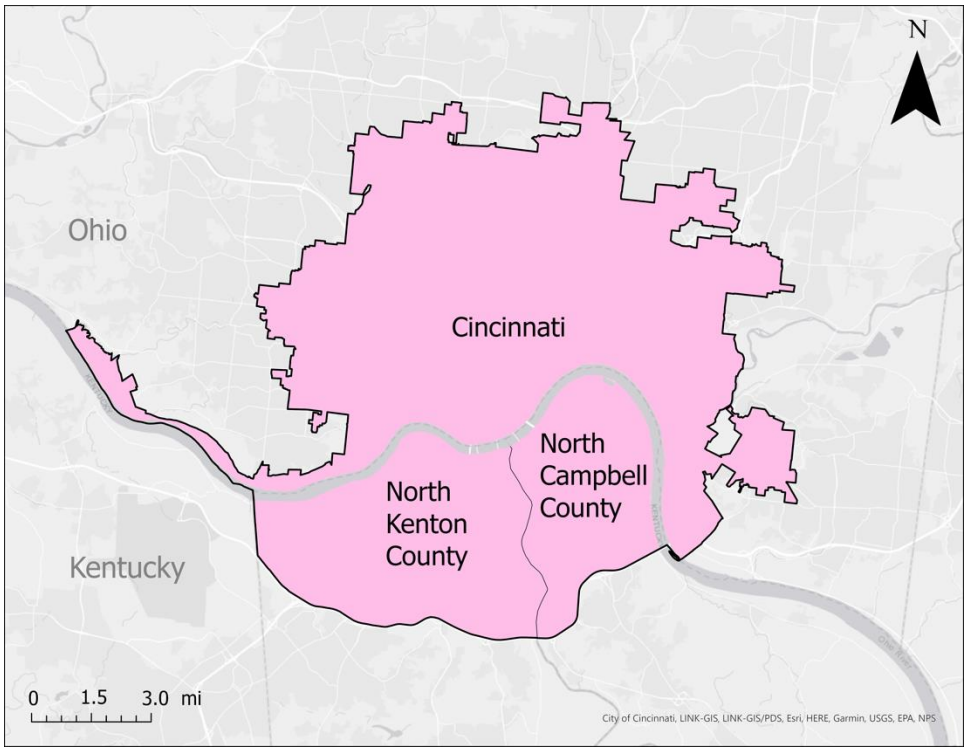

Figure 1. Study area map showing Cincinnati, OH, North Kenton County, and North Campbell County, KY.

3. Methodology

3.1 Data Acquisition

Earth observation data were acquired from 2004 to 2021. Global Precipitation Measurement (GPM) Integrated Multi-satellitE Retrievals for GPM (IMERG) was used in Google Earth Engine (GEE) to retrieve precipitation data for the InVEST Urban Flood Risk Mitigation Model (Table 1). Landsat 8 Operational Land Imager (OLI) and Thermal Infrared Sensor (TIRS) were used to calculate a normalized difference vegetation index (NDVI) as a landslide susceptibility factor.

Table 1

Description of Earth observations used in data processing

Platform	Sensor	Product ID	Dates	Purpose	Source
GPM IMERG	N/A	NASA/GPM_L3/IMERG_V06	January 1st 2004 – December 31st 2020	Gather precipitation reference data for the InVEST input	GEE
Landsat 8 OLI	OLI /TIRS (2 Bands: Red, Near-infrared)	LANDSAT/LT05/C01/T2_SR USGS Landsat 5 Surface Reflectance Tier 2	January 1st – December 31st 2020	Calculate the change in NDVI as a landslide susceptibility factor	GEE

Several ancillary datasets were used to map landslide susceptibility and exposure. The USGS National Elevation Dataset 3D Elevation Program (3DEP) was used to obtain a 1/9th arc-second digital elevation

model (DEM) for slope analysis. Lithology data used to assess landslide susceptibility were derived from the 2017 USGS State Geologic Compilation Map, while clay percent data was obtained from the USDA Soil Survey Geographic (SSURGO) Database. Shapefiles of major highways and interstates within the study area were obtained from the US Census TIGER/Line collections. The landslide inventories used for validation of the susceptibility map were obtained from the USGS and Kentucky Geological Survey. Human population characteristics used for exposure mapping were obtained from the US Census.

The InVEST Urban Flood Risk Mitigation Model requires numerous inputs including a watershed vector, depth of rainfall event in millimeters, a raster map of soil hydrological groups, a land cover raster map, and a biophysical table containing curve numbers of the study area's soil types associated to land cover classes. The InVEST model also allows the input of two optional files, a built infrastructure vector and a damage loss table containing infrastructure categories and their associated economic value. These optional inputs would produce a flood risk service output. The team utilized the United States Department of Agriculture (USDA) Gridded Soil Survey Geographic (gSSURGO) soil type and drainage class datasets for the study area to determine curve number calculations. To create the biophysical table and map land cover within the study area watersheds, the team used the 2010 USA National Land Cover Database (NLCD) Land Use Land Cover (LULC) raster dataset. The team chose to use the 2010 version of the NLCD data as it was more temporally consistent with other ancillary datasets' time range. Additionally, the Ohio-Kentucky-Indiana (OKI) Regional Council of Governments and Kenton County's Planning and Development Services provided building footprint shapefiles which the team used to calculate built infrastructure presence within the study area. Lastly, Climate Hazards Group InfraRed Precipitation with Station data (CHIRPS) was accessed from GEE and was used in a case study to assess rainfall variability across the study area.

3.2 Data Processing

3.2.1 Data Processing for InVEST Urban Flooding Model

To prepare for the computation of the InVEST model's runoff retention and runoff value outputs, the team adjusted ancillary datasets to match the attributes of the Cincinnati and Covington area. The model required an input for depth of rainfall in millimeters, which was derived by the team referencing specific storm events known to have caused flooding in the study area. This was determined using GPM IMERG data in GEE. Storm sizes of 60mm, 90mm, 120mm, and 150mm were chosen to approximate different depths of rainfall events to determine a range of rainfall causing flooding in the region.

The raster map of soil hydrological groups required conversions from each hydrological group, type A, B, C, or D, to be classified in accordance with pixel values of 1, 2, 3, or 4. The USDA Gridded Soil Survey Geographic datasets included the types of soils and classes within the study area, however some of the urbanized soils were unlabeled. To supplement this data, the USDA SSURGO Database and the Natural Resources Conservation Service's (NRCS) engineering handbook were referenced to determine each soil's hydrological group. For each soil hydrological group, A, B, C, and D, the associated runoff curve number determined by the NRCS for each LULC type was input to the biophysical table, predicting the soil's infiltration capacity and runoff potential. The Soil Conservation Service (SCS) curve number method is used to approximate runoff from a rainfall event in a particular area, based on the area's hydrological soil group, land use, and hydrologic condition (United States Department of Agriculture, 2009). The SCS curve numbers and associated NLCD LULC classes are shown in Table A1 of the Appendix.

The LULC raster dataset was clipped to the study area and LULC classes were combined to produce ten main LULC types: open developed land with < 20% impervious surface, low intensity developed land with 20 – 49% impervious surface, medium intensity developed land with 50 – 79% impervious surface, high intensity developed land with 80 – 100% impervious surface, open water, wetlands, forests, shrub and grasslands, agricultural fields, and barren land (Figure 2). Non-urbanized areas have pervious surfaces to allow for water to be absorbed into the ground. Assessing the LULC class distribution throughout the study area helped to validate the runoff retention and runoff values determined with the InVEST Urban Flood Risk Mitigation Model based on land use trends.

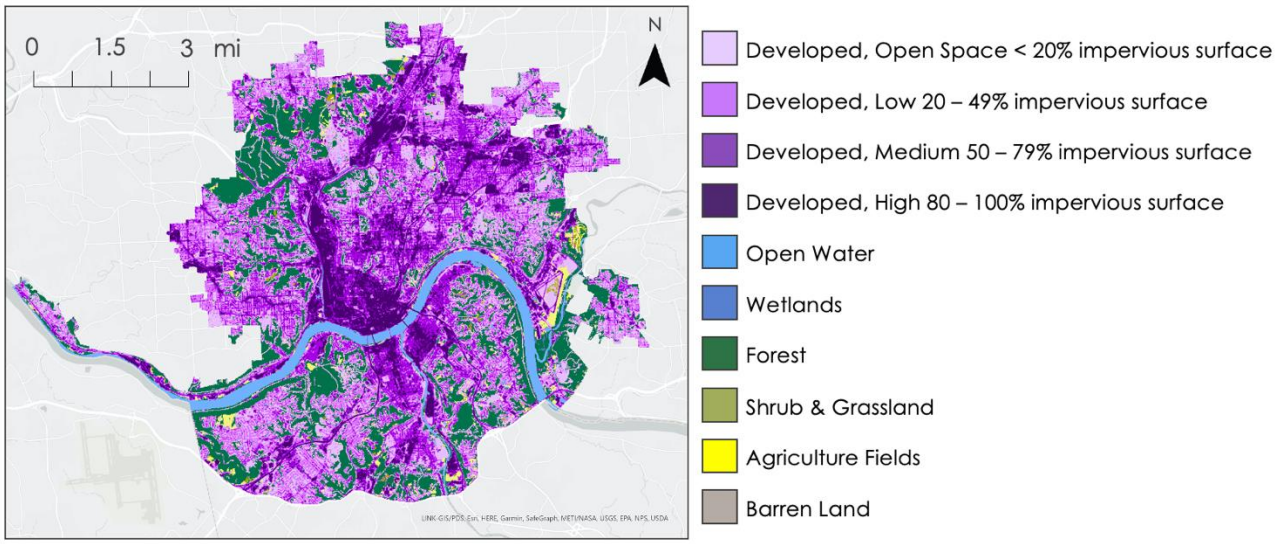

Figure 2. Map of the spatial distribution of LULC classes within the study area from the 2010 NLCD dataset. The urbanized areas were categorized by varying levels of purple from light to dark. The darkest purple shows the most developed areas with the highest percentage of impervious surfaces, mostly consisting of buildings, roads, and commercial and industrial complexes. The dark green to yellow areas were categorized by greenery, such as forests, wetlands, shrub and grasslands, and agriculture fields.

3.2.2 Data Processing for Landslide Susceptibility and Exposure

To create a landslide susceptibility map, the team applied information value models to datasets of landslide factors applicable to the study area. The vector datasets were projected in NAS 1983 StatePlane Ohio South FIPS 3402, with the raster datasets being projected in NAD 1983 UTM Zone 16N using ArcGIS Pro. All data sets were clipped to match the extent of the study area.

The factors assessed in the landslide susceptibility mapping include elevation, slope, roughness, lithology, clay percent, distance to roads, and absolute change in NDVI (δNDVI). The two 1/9th arc-second DEMs obtained from 3DEP were edge matched and placed in a mosaic that covered the entire study area. The team filled this raster using ArcGIS Pro Analyst Tools to ensure there were no sinks in the dataset. Then the team ran the DEM through the Slope Spatial Analyst tool that identified the steepness between the cells in the raster to create a slope layer. Finally, a Focal Statistics tool was used to create the roughness raster. Each cell reports the number of unique slope values within its neighborhood, which serves as a proxy for roughness. Clay percent was obtained using the USDA Soil Survey Geographic Database which provided tabular and spatial tables of clay percent by soil type for the study area. To calculate the strength of each geologic unit within the lithology layer, the team used ArcGIS Pro's Zonal Statistics tool on the landslide inventory and geologic map. The strength value assigned to the rock type was equal to the number of landslides that occurred within the rock layer normalized by the rock layers area. The Euclidean Distance tool was used to create the distance to roads raster layer from the road lines dataset. Finally, a δNDVI raster was created in GEE using Landsat 8 OLI and TIRS imagery of the study area from 2013 and 2020.

To produce a landslide susceptibility map, the variables were input into a fuzzy membership model (Figure B1), which reclassified the values from 0, representing no landslide association, to 1, representing very high landslide association (Table B1). The resulting reclassified layers were then input into a fuzzy overlay model to produce a final landslide susceptibility map. Finally, the landslide susceptibility map was reclassified into five categories representing very low, low, moderate, high, and very high susceptibility. The cutoffs were based on previous work done by the Dominican Republic Disasters Summer 2019 DEVELOP team (Aldama

et al., 2019). These categories represented the 50th, 75th, 90th, and 95th percentiles of susceptibility, respectively.

Landslide exposure maps were created by combining the final susceptibility data with vulnerable demographic information obtained from census block groups. The landslide susceptibility for each census block group was determined by finding the average value of the susceptibility raster within each polygon of the layer. The vulnerable demographic information was obtained by clipping the census block group data to the study area and extracting the population density of the socio-economic groups that were determined to have higher vulnerability to landslides. At partner request, the demographics chosen for the exposure analysis were the densities of African American populations, elderly residents greater than 85 years old, and impoverished populations. Census block group neighborhoods at the intersections of high landslide susceptibility and high socioeconomic variable were classified as high exposure.

3.3 Data Analysis

3.3.1 Data Analysis for the InVEST Urban Flood Risk Mitigation Model

To validate the InVEST model's output maps displaying runoff retention and runoff values, the team utilized the LULC map. As InVEST relies on the association of LULC to soil hydrological groups and their SCS curve numbers, the team was able to interpret runoff values and runoff retention values both in different LULC classes as well as in their entirety for each storm event. Impervious surfaces, highly prevalent in urbanized areas, have almost zero runoff retention capacity which leaves the opportunity for rainfall to overflow across the landscape. Depending on the storm size, the water's inability to seep into the surface increases the likelihood of runoff transitioning into a flood hazard. In contrast, greenery within the study area had a positive effect to combat these hazards. Vegetated land cover allowed for stormwater to infiltrate the soil, therefore, decreasing the amount of runoff based on a given storm size. The other land cover classes within the map have their associated retention and runoff capacities taken into account, however the impervious surface and vegetative land cover present the most significant impact in flood-based scenarios. Understanding the characteristics of these types of land covers is necessary when assessing the areas flooding susceptibility.

3.3.2 Optional InVEST Outputs

As part of the project analysis, the team chose to include a built infrastructure vector and a damage loss table to produce the InVEST Urban Flood Risk Mitigation Model's optional outputs. The built infrastructure vector included polygons of all buildings within the study area, including impervious surfaces such as roads. All infrastructure needed to be categorized into one of five types: residential, commerce, industry, infrastructure, or agriculture (Huizinga et al., 2017). The associated damage loss table identified damage costs, in dollars per square meter, to assess the costs of flood damages impacting built infrastructure. This additional analysis was ultimately not pursued beyond a test run to determine the output values.

3.3.3 Data Analysis for Landslide Susceptibility and Exposure

The team used a frequency ratio analysis to validate the landslide susceptibility map. For this approach, landslide polygons from the Kentucky Geological Survey were first converted into a point layer and merged with the landslide point layer from the USGS. Any landslide locations found in both datasets were only counted once. Then the landslide susceptibility raster layer was classified into quantiles, representing very low, low, medium, high, and very high susceptibility. The Extract Values to Points tool in ArcGIS Pro was used to count the number of landslides in each category. Next, the number of pixels in each category were extracted. The Landslide Ratio was obtained by dividing the number of landslides in each category by the total number of landslides in the region. Likewise, the Pixel Ratio was calculated by dividing the number of pixels in each category by the total number of pixels in the region. Finally, the Frequency Ratio was obtained by dividing the Landslide Ratio by the Pixel Ratio. Frequency Ratios greater than 1 indicate strong relationships between landslide occurrence and susceptibility, suggesting that the landslide susceptibility map is valid.

To display landslide exposure, the average value of the landslide susceptibility raster had to be found for each census block group. This process was performed using the Zonal Statistics tool on ArcGIS Pro, which allowed for the susceptibility raster to be calculated per census block polygon. The resulting statistics were then added into the census block attributes table for the study area, which allowed for each vulnerable population to be displayed relative to susceptibility. In relation to total population, ratios for African American, impoverished, and elderly populations were created before being combined to produce an overall vulnerability index.

4. Results & Discussion

4.1 InVEST Results

4.1.1 Runoff and Runoff retention

To approximate the impacts of different storm events on the study area, the InVEST Urban Flood Risk Mitigation Model was run using daily rainfall inputs of 60mm, 90mm, 120mm, and 150mm. The team calculated and defined runoff and runoff retention values based on the documentation of the InVEST Urban Flood Risk Mitigation Model (Stanford Natural Capital Project, 2021b). The resulting runoff raster datasets and runoff retention raster datasets indicated a consistent maximum of 90% rainfall retention between the 60mm, 90mm, and 120mm daily rainfall storm events. However, the 150mm storm event indicated a maximum runoff retention of 89%, suggesting the study area's capacity for retaining rainfall was decreasing with the growing storm events. For clarity, the team chose to focus on the 60mm daily rainfall storm event and the 150mm daily rainfall storm event and compared the resulting raster datasets to understand flooding variability across different storms.

The runoff retention and runoff values are presented in Figure 3 as a percentage of total rainfall for a 60mm (2.3 inches) daily rainfall storm event. The runoff retention map (Figure 3a) indicates greater capacity for runoff retention in the darker blue shades, while lighter areas represent little to no capacity for the area to retain rainfall as they are correlated to the highly developed LULC classes. The Northwest corner of the runoff retention map represents the Mt. Airy Forest, an area with approximately 90% runoff retention during the 2.3-inch storm event. In the runoff map (Figure 3b), light areas of low rainfall runoff correspond to vegetated LULC classes including forests, grasslands, and agriculture. Regions of high runoff are consistent with the areas of low runoff retention, primarily the highly urbanized neighborhoods, Queensgate, and Over-the-Rhine, in downtown Cincinnati and northern Covington.

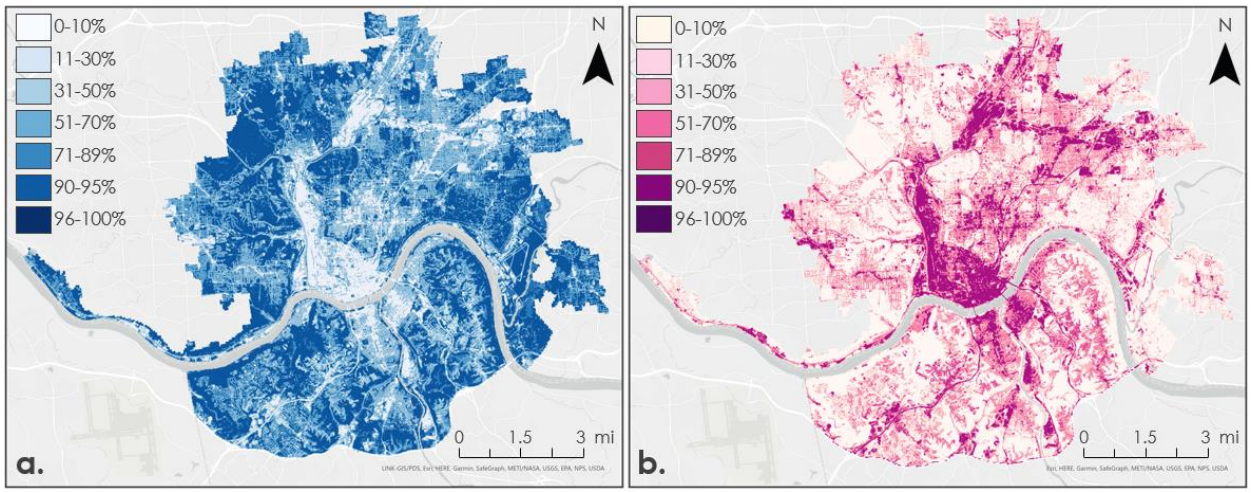

Figure 3. Outputs from the InVEST Urban Flood Risk Mitigation Model. (a) Runoff retention displayed in shades of blue and (b) runoff values displayed in shades of pink are both displayed as percentages of the 60-mm (2.3-inch) daily rainfall event. Values are measured in percentages of total rainfall from light, 0%, to dark, 100%. Note that runoff retention and runoff values (expressed as a percent of rainfall) add up to 100%,

The 150mm, or 6-inch, daily rainfall storm event (Figure 4) indicates increased stress placed on the study area, with lower total capacity for rainfall retention and higher rainfall runoff values. While the runoff retention values in the 2.3-inch storm event ranged to 90% rainfall retention, the maximum retained runoff in the 6-inch storm event was 89%. The 6-inch storm event runoff retention map (Figure 4a) displays noticeably lighter values than the 2.3-inch storm event retention map (Figure 3a). When directly comparing the two runoff retention maps (Figure C1) there is a clear reduction in the capacity for even the highest contributing retaining LULC classes to absorb the daily rainfall. Exact data reflecting rainfall runoff retention per LULC class can be found in Table D1.

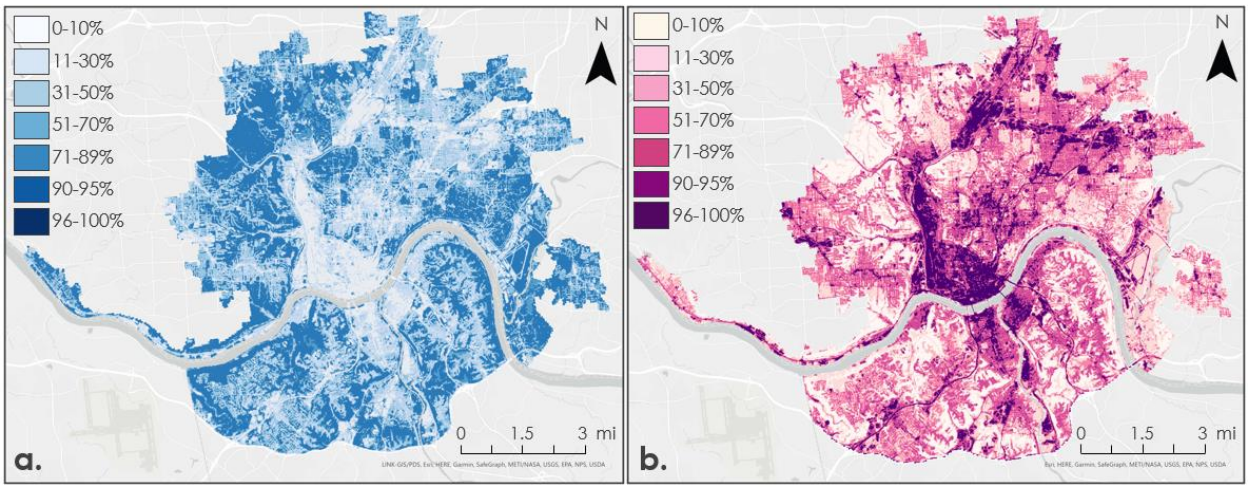

Figure 4. Outputs from the InVEST Urban Flood Risk Mitigation Model. (a) Runoff retention and (b) runoff values are displayed as percentages of the 150-mm(6-inch) daily rainfall event. Values are measured in percentages of total rainfall from light, 0%, to dark, 100%. Runoff retention (a) is displayed in shades of blue, and runoff (b) is displayed in shades of pink.

Rainfall runoff mapped for the 6-inch daily storm event (Figure 4b) indicates a greater proportion of this larger storm event was ultimately runoff; consistent with the reduced capacity for the study area to retain increased rainfall. While vegetated areas such as forests, grasslands, and agricultural lands had 0 – 10% runoff in the 2.3-inch storm event (Figure 3b) these same areas now indicate up to 50% runoff with the increased rainfall event (Figure 4b). Highly developed, downtown urban areas produced 96 – 100% runoff in the 6-inch daily storm event and can be clearly seen producing a greater percentage of runoff than in the 2.3-inch daily storm event (Figure C2). Exact data reflecting rainfall runoff values per LULC class can be found in Table D1.

By definition, the sum of runoff retention and runoff values is 100%. Thus, regions with high values in the runoff retention maps display positive aspects of the region's land cover in its ability to retain stormwater, while regions with high values in the runoff value maps demonstrate the region's local infrastructure and impervious surfaces that contribute to high stormwater runoff. Since the InVEST Urban Flood Risk Mitigation Model assesses flood risk based on land cover type and associated soil curve numbers, the results were able to be determined per land cover class for each storm event (Table D1). The runoff retention maps for both daily rainfall events demonstrate that forests provide the highest retention capacity, retaining the highest percentage of rainfall throughout both model runs. The urban areas were increasingly unable to retain stormwater as impervious surface percentage increased. Overall, the vegetated regions such as forests, wetlands, grass and shrublands, and agricultural fields were the most beneficial land cover types contributing to stormwater retention in the study area. Consistent with the runoff retention per land cover class, the runoff per landcover class indicates little ability to increasingly developed areas to retain stormwater. Runoff was very low in the forested areas, with similar lower values shown in the wetlands, grass and shrublands, and agricultural lands.

4.1.2 Rainfall Accumulation Case Study

An additional case study was conducted to assess how rainfall accumulation varied across the study area during a storm. The NASA Earth observation satellite GPM IMERG was applied to this study in GEE. However, the Cincinnati and northern Covington study area bounds were too small within GPM IMERG's 0.1-degree, 10-kilometer, resolution. Instead, Climate Hazards Group InfraRed Precipitation with Station data (CHIRPS) was used. CHIRPS is a dataset by the University of California Santa Barbara that provides gridded rainfall estimates derived from rain gauge data and satellite observations.

At a resolution of 0.05-degrees, CHIRPS allowed for rainfall variability to be seen within the study area for recorded storm sizes of 60mm, 87mm, and 128mm (Climate Hazards Center of UCSB, 2021). Two 60mm storms measured within the study area show high rainfall variability within a similar storm size (Figure E1a, b). In the 87mm storm event a majority of the area only received rainfall up to 37mm (Figure E1c). The 128mm storm size event is the largest recorded within the study period and spread across the entire state (Figure E1d). The minimum pixel value recorded was 74mm and the maximum was 128mm.

4.1.3 Errors and Uncertainties

The InVEST Urban Flood Risk Mitigation Model intends to calculate flood volume, runoff, and runoff retention per watershed within a given study area. The highest resolution hydrologic unit codes for this region were significantly larger than was useful for our analysis, so the team input the whole study area as a single watershed. The team was able to gather sewershed vector data for Hamilton County, which allowed an InVEST model run determining flood volume values per sewershed, and provided data determining more precise threats to different neighborhoods. However, this data was only available for Hamilton County, and the precise sewershed analysis could not be completed for the Kentucky side of the study area. The lack of precise watershed data made it difficult to determine specific neighborhoods of concern within the region.

4.2 Landslide Susceptibility and Exposure Results

4.2.1 Landslide Susceptibility Results

Drawing on the 2019 Dominican Republic Disasters Summer 2019 DEVELOP team's methodology (Aldama et al., 2019), the final landslide susceptibility map was reclassified into five categories of susceptibility, drawn from the 50th, 75th, 90th, and 95th percentile breaks in the data (Figure 5). Areas of highest susceptibility are along major routes like U.S. Route 50, which includes Columbia Parkway, along with Mary Ingles Highway and Kentucky Route 8. Meanwhile. Contrastingly, centrally located urban areas like downtown Cincinnati and Covington, show a much lower propensity for landslides.

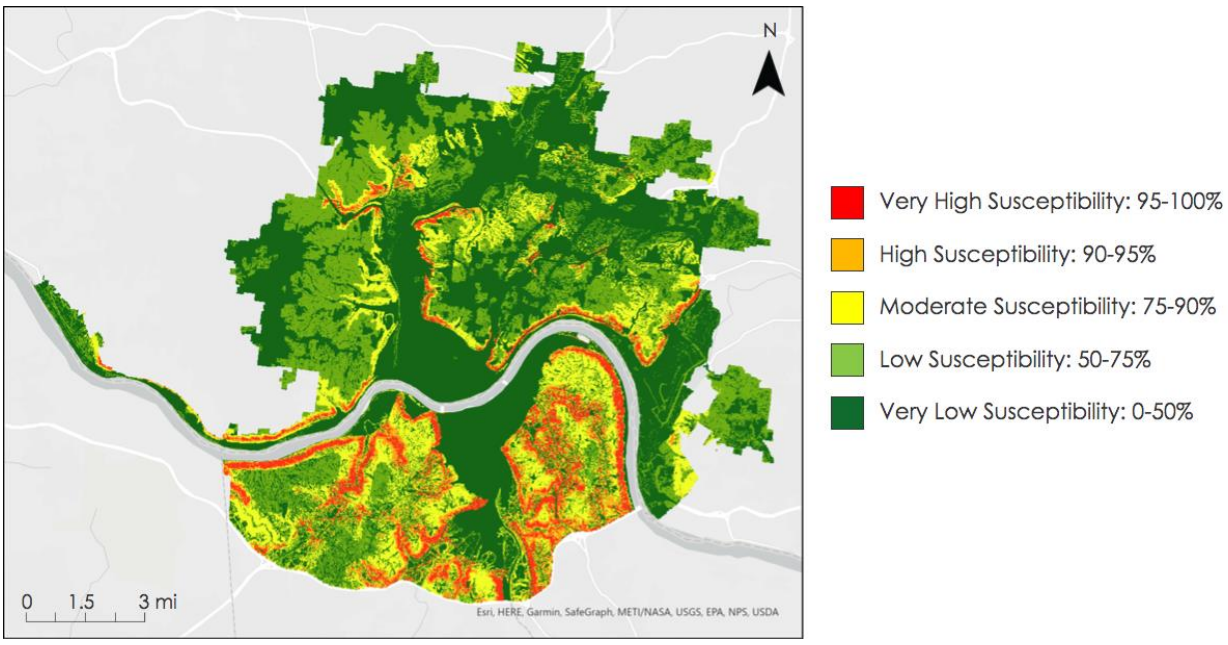

Figure 5. The landslide susceptibility map highlights areas of differing susceptibility to hazardous landslide events in the study area. Dark green corresponds to very low susceptibility (below the 50th percentile of quantified susceptibility), light green to low susceptibility (between the 50th and 75th percentile), yellow to moderate susceptibility (between the 75th and 90th percentile), orange to high susceptibility (between the 90th and 95th percentile), and red to very high susceptibility areas (95th percentile and above).

The susceptibility map was validated by a spatially-explicit inventory of 125 landslides derived from the USGS and Kentucky Geological Survey (Figure F1). A frequency ratio analysis showed ratios greater than 1 starting in the 'moderate' susceptibility category (Figure F2). The steeply increasing trend of ratios shows that, adjusted for each category's area on the map, the 'very high' susceptibility category captures the most landslide events, followed by the 'high' category, and progressing accordingly down the x-axis. This strong performance on historical data suggests that the landslide susceptibility map is accurate and given the propensity for mass wasting events to reoccur under similar conditions, the map emphasizes areas of current concern.

While seven variables were applied to the fuzzy overlay model to create the final landslide susceptibility map (slope, elevation, roughness, clay percent, δNDVI, lithology, and distance to roads), several others were considered and, likely, many more could have contributed meaningfully to the model. The team hypothesized that LULC would capture the negative impact of vegetation on landslide occurrence; the tensile strength of roots in forested and highly vegetated areas is known to inhibit slope failure. However, when the team assessed the LULC raster with a frequency ratio analysis, the data showed the opposite trend. The team also observed this with NDVI data at first attempt, whose frequency ratios suggested that highly vegetated areas experienced more landslides on average. Likely, areas favored for urban development and subsequently deforestation had lower inclines that made the area more hospitable. Therefore, slope boasted the highest frequency ratio, making it the strongest predictor of landslides among the considered variables. Slope was likely being conflated with vegetation density and biasing NDVI and LULC's associations with landslide occurrence. To minimize such bias, the team elected to include δNDVI in lieu of raw NDVI values. This captured vegetation disturbance, serving as a proxy for recent human activity that can leave an area landslide prone, and it yielded frequency ratios more consistent with trusted literature.

Similarly, it was hypothesized that landslide frequency would increase inversely with distance to roads, given that the region has had many reported landslide events along major roads and highways. The initial analysis, which included most roads in the study area, showed no association between the two variables. Interestingly,

when the team opted for a coarser resolution, calculating Euclidean distance from highways and state routes, the frequency ratio analysis revealed a meaningful trend consistent with literature and initial hypotheses. The DEM was crucial for deriving elevation, slope, and roughness to include in the fuzzy logic model.

Out of the seven variables included in the final susceptibility map, slope was found to be the most important factor for predicting landslide susceptibility. The frequency ratio analysis for slope showed the strongest relationship between increasing susceptibility category and increasing normalized landslide occurrence. This justifies the separate application of slope in the fuzzy overlay model. Furthermore, steep slopes are prominent on roadways along the Ohio River where high historical landslide incidence has been observed.

4.2.2 Landslide Exposure Results

The final combined landslide exposure map (Figure 6) visualized the combined average of three socioeconomic populations with landslide susceptibility per block group in a bivariate display. High exposure to African American (Figure G1) and impoverished populations (Figure G2) were seen to have larger concentrations on the Cincinnati side of the Ohio River; however, this may have been the result of higher census populations recorded in the Cincinnati area compared to Northern Kentucky. Exposure to elderly populations (Figure G3) appeared to be more evenly spread between the two states with only marginally higher landslide exposure for the elderly displayed on the Kentucky side of the river. Unsurprisingly, heavily urbanized areas like downtown Cincinnati and Covington had extremely low landslide exposure due to lower landslide susceptibility from a lack of geological factors that contribute to landslides. The combined exposure map highlighted areas around the Cincinnati neighborhoods of Avondale, Mt. Airy, North Fairmount and South Fairmount as having both high landslide susceptibility and high socioeconomic vulnerability. Pockets of high landslide exposure were displayed in the home rule cities of Kenton Vale and Crescent Springs in northern Kentucky.

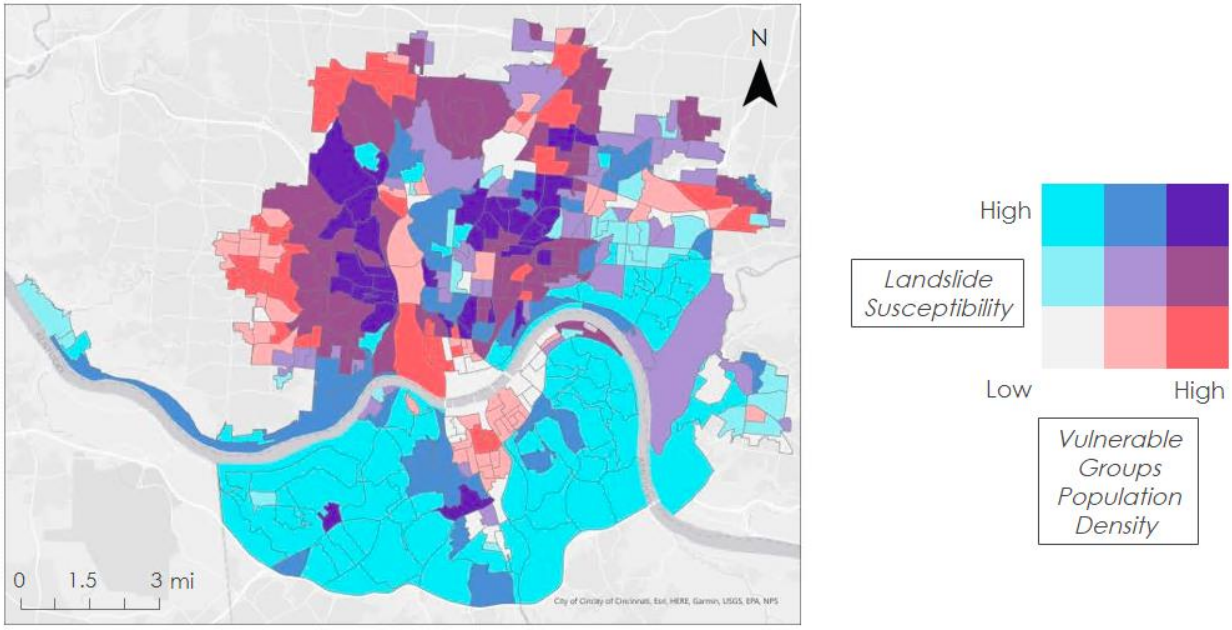

Figure 6: The landslide exposure map shows the amalgamation of landslide susceptibility and combined vulnerable population densities in a bivariate color scheme. Blue was chosen to represent landslide susceptibility in each of the exposure maps produced. The bivariate display created darker areas where susceptibility and vulnerable population density were the highest. This allows for both landslide susceptibility and vulnerability to be displayed simultaneously, with darker purple areas on the map representing areas of high landslide exposure.

4.2.3 Errors and Uncertainties

Errors and uncertainties for the landslide susceptibility and exposure portion of the project were primarily due to the landslide inventory and the lithology layer. While the landslide inventory used for the frequency ratio analysis was derived from two separate inventories, there is still a possibility that landslide locations were unrecorded. Since the validation process analyzes the number of landslides that occurred within each susceptibility category, a non-exhaustive inventory that undercounts landslides in some regions could misrepresent the map's performance. A similar effect would be observed with inaccurate occurrence locations. If a landslide point was erroneously reported in a different susceptibility category, our validation process would record a different level of confidence for our map. For the lithology layer, the errors and uncertainties arose from assumptions on each rock unit's susceptibility. Since the fuzzy overlay model relied on numerical inputs, the lithology layer needed to report relative landslide susceptibility and not the geological unit's name. To do this conversion, the calculated the number of landslides that occurred within each rock type and used that value to calibrate risk. However, if the rock layers were improperly mapped or the landslide inventory was non-exhaustive, these risk values would be incorrect. While this method did classify rock types known to be more landslide prone as having higher levels of landslide susceptibility, a susceptibility-assignment methodology that is less reliant on the potentially imprecise landslide inventory and geologic map would be more ideal.

4.3 Future Work

One limitation of the InVEST Urban Flood Risk Mitigation Model is the inability to consider riverine flooding during storm events. As the Ohio River crosses the center of the study area and divides two major urban centers, riverine flooding should be assessed as part of future work considering stormwater flooding within the region. Additionally, the model specifies the simple nature of using SCS curve numbers for predicting soil capacity to retain stormwater. Future analyses should consider more complex statistical approaches to deriving curve numbers for more precise runoff and runoff retention values.

The landslide susceptibility and exposure maps created for this project were static. In the future, a team could use a model, like the Landslide Hazard Assessment model for Situational Awareness (LHASA) model, to develop a real-time landslide susceptibility map. LHASA works by incorporating current precipitation conditions alongside a static landslide susceptibility map to highlight areas most susceptible to slope failure. This product would allow Groundwork ORV and Groundwork USA to alert community members of heightened landslide risk, as well as gather data on which areas are experiencing frequent alerts. This latter metric could be useful in informing the organizations' outreach and education programs. Additionally, future work could focus on creating new exposure maps to further highlight the region's landslide vulnerability. Additional exposure maps could analyze other population characteristics to investigate whether these variables intersect with landslide susceptibility and to establish a more comprehensive exposure analysis. Exposure maps could also include critical infrastructure, like hospitals, schools, and bridges, in order to analyze how landslides would impact city services. Finally, future work on landslide susceptibility and exposure mapping could integrate remote sensing data to identify unmapped landslide occurrences. While the inventory compiled from the USGS and Kentucky Geological Survey recorded 125 landslides in the region, increasing the number of observations would lend more statistical significance to the validation process. This would especially be useful in the Ohio portion of the study area, as the landslide inventory is less exhaustive than in Kentucky.

5. Conclusions

Using the InVEST Urban Flood Risk Mitigation Model, the team determined that in storms affecting the area, highly urbanized land cover types retained barely 10% of rainfall, while forested areas retained up to 90% of rainfall. Runoff directly increased as percentage of impervious surface increased, indicating urban neighborhoods with little greenspace face the greatest risk of flooding. The downtown Cincinnati, Queensgate, and Over-the-Rhine neighborhoods retained the least amount of rainfall, between 10 – 15% across the measured daily rainfall events.

The static landslide susceptibility map identified key areas facing heightened landslide susceptibility. Specifically, steep slopes near major roads, like US Routes 50 and 72 in Ohio, and Kentucky Route 8, have very high landslide susceptibility. The validation frequency ratio analyses found that slope was the most predictive variable for determining landslide susceptibility in the region. The landslide exposure maps showed many intersections between areas of high socioeconomic vulnerability and high landslide susceptibility. The communities at these intersections may be less resilient to landslide events, and the intersections themselves may reflect broader underlying conditions that influence where people may live. Three neighborhoods with high landslide exposure include the areas around Avondale, North Fairmount, and South Fairmount.

6. Acknowledgments

The Cincinnati and Covington Urban Development II team would like to thank our project partners at Groundwork USA and Groundwork ORV for their support and collaboration: Cate Mingoya, Lawrence Hoffman, Sarah Morgan, and Tanner Yess. The team would additionally like to thank Dr. Cedric Fichot, Dr. Kenton Ross, and Dr. Matthew Crawford for their guidance throughout this term. We would also like to thank our NASA DEVELOP Fellow Celeste Gambino for her guidance and support throughout this term. Finally, thanks to the previous NASA DEVELOP Cincinnati and Covington Urban Development Team members Olivia Cronin-Golomb, Samuel Feibel, and Katrina Rokosz.

Any opinions, findings, and conclusions or recommendations expressed in this material are those of the author(s) and do not necessarily reflect the views of the National Aeronautics and Space Administration.

This material is based upon work supported by NASA through contract NNL16AA05C.

7. Glossary

DEM – Digital Elevation Model: a representation of the Earth's topography, excluding surface objects such as trees or buildings.
Earth observations – Satellites and sensors that collect information about the Earth's physical, chemical, and biological systems over space and time.
GPM – Global Precipitation Measurement: a NASA earth observation satellite that measures both active precipitation and atmospheric conditions.
gSSURGO – USDA Gridded Soil Survey Geographic: an Environmental Systems Research Institute, Inc. (Esri®) file geodatabase that contains soil geographic data derived from Soil Survey Geographic Database.
IMERG – Integrated Multi-satellitE Retrievals for GPM: an algorithm that uses GPM imagery to calculate precipitation amounts over the Earth's surface.
InVEST – Integrated Valuation of Ecosystem Services and Tradeoffs: a suite of models used to map and evaluate the changes in ecosystems influencing natural goods and services that sustain human life.
NDVI – Normalized Difference Vegetation Index: a dimensionless metric that can be used to measure the density of green vegetation on the Earth's surface.
OLI – Operational Land Imager: an instrument within the Landsat 8 satellite that measures visible, near-infrared, and short-wave infrared light that is reflected from the Earth's surface.
TIRS – Thermal Infrared Sensor: an instrument within the Landsat 8 satellite that measures the Earth's land surface temperature.

8. References

Aldama, S., Dandridge, C., Kim, K., Pavur, G. (2019). *Dominican Republic disasters: Mapping landslide susceptibility and exposure in the Dominican Republic using NASA Earth observations.* NASA DEVELOP National Program. https://develop.larc.nasa.gov/2019/summer/DominicanRepublicDisasters.html

Cincinnati Department of Transportation and Engineering. (2019). *2019 Columbia Parkway Landslide Report*. 1–33.

Climate Hazards Center of UCSB. (2021). CHIRPS: Rainfall Estimates from Rain Gauge and Satellite Observations | Climate Hazards Center - UC Santa Barbara. https://www.chc.ucsb.edu/data/chirps

Fleming, R.W. & Taylor, F.A. (1980). Estimating the Costs of Landslide Damage in the United States, U.S. Geological Survey

Hansen, M. (1995). Landslides in Ohio. *Geo Facts Ohio Department of Natural Resources, 8*, 1-2. https://ohiodnr.gov/static/documents/geology/GF8_Hansen_1995.pdf)

Huffman, G.J., Stocker, E.F., Bolvin, D.T., Nelkin, E.J., & Tan, J. (2019). GPM IMERG Final Precipitation L3 1 month 0.1 degree x 0.1 degree V06, Greenbelt, MD, Goddard Earth Sciences Data and Information Services Center (GES DISC), Accessed 2019-10-08. doi: 10.5067/GPM/IMERG/3B-MONTH/06

Huizinga, J., Moel, H. de, Szewczyk, W. (2017). *Global flood depth-damage functions. Methodology and the database with guidelines*. EUR 28552 EN. doi: 10.2760/16510

Hong, Y., Adler, R., & Huffman, G. (2006). Evaluation of the potential of NASA multi-satellite precipitation analysis in global landslide hazard assessment. *Geophysical Research Letters*, *33*(22), 1-5. doi: 10.1029/2006GL028010

Liu, W., Feng, Q., Chen, W., & Deo, R. C. (2020). Stormwater runoff and pollution retention performances of permeable pavements and the effects of structural factors. *Environmental Science and Pollution Research*, *27*, 30831-30843. doi:10.1007/s11356-020-09220-2

Mardon, S. (2020). Landslide Hazards in Kentucky. Kentucky Geological Survey. https://www.uky.edu/KGS/education/factsheet/landslide_factsheet.pdf

Riestenberg, M. M., & Sovonick-Dunford, S. (1983). The role of woody vegetation in stabilizing slopes in the Cincinnati area, Ohio. *Geological Society of America Bulletin*, *94*(4), 506-518. doi:10.1130/0016-7606(1983)94<506:TROWVI>2.0.CO;2

Sarkar, S., and D. P. Kanungo. (2004) An Integrated Approach for Landslide Susceptibility Mapping Using Remote Sensing and GIS. *Photogrammetric Engineering & Remote Sensing*70(5), 617–25.doi:10.14358/PERS.70.5.617.

Sparling, H., & DeMio, T. (2019, March 6). 'It's like someone put a bomb in your yard.' Landslides in Greater Cincinnati are bad. And they'll probably get worse. *Cincinnati Enquirer*. https://eu.cincinnati.com/story/news/2019/03/05/landslides-climate-change-bring-more-cincinnati/2931026002/

Stanford Natural Capital Project. (2021a, June 3). InVEST. Natural Capital Project. https://naturalcapitalproject.stanford.edu/software/invest

Stanford Natural Capital Project. (2021b). *InVEST Documentation: Urban Flood Risk Mitigation model.* Retrieved from https://invest-userguide.readthedocs.io/en/latest/urban_flood_mitigation.html.

Riestenberg, M. M., & Sovonick-Dunford, S. (1983). The role of woody vegetation in stabilizing slopes in the Cincinnati area, Ohio. *Geological Society of America Bulletin*, *94*(4), 506-518. doi:10.1130/0016-7606(1983)94<506:TROWVI>2.0.CO;2

United States Department of Agriculture (USDA) (2009). Chapter 7: Hydrologic soil groups in *National Engineering Handbook: Part 630 - Hydrology.*

U.S. Geological Survey Earth Resources Observation and Science Center. (2014). Landsat 8 OLI Level-2 Surface Reflectance (SR) Science Product [Data set]. U.S. Geological Survey. https://doi.org/10.5066/f78s4mzj

U.S. Geological Survey Earth Resources Observation and Science Center Archive. (2013). Landsat 8 OLI/TIRS Level-2 Data Products Surface Reflectance [Data set]. U.S. Geological Survey. https://doi.org/10.5066/f78s4mzj

Validity and Effectiveness of Landslide Susceptibility Maps. (2004). Marshall College. https://www.marshall.edu/cegas/geohazards/2004pdf/Session%205/Pohana-Cincinnati.pdf

Van Westen, C. J., Castellanos, E., & Kuriakose, S. L. (2008). Spatial data for landslide susceptibility, hazard, and vulnerability assessment: An overview. *Engineering Geology, 102*(3-4), 112-131. https://doi.org/10.1016/j.enggeo.2008.03.010

9. Appendices

Appendix A

Table A1
SCS curve numbers and their associated NLCD LULC classes. For a description of how the curve numbers are used in the InVEST Urban Flood Risk Mitigation Model, see documentation online at https://invest-userguide.readthedocs.io/en/latest/urban_flood_mitigation.html (Stanford Natural Capital Project, 2021).

NLCD LULC Type	**Soil Curve Numbers**			
LULC Description	Hydrological Group A	Hydrological Group B	Hydrological Group C	Hydrological Group D
Open Water	100	100	100	100
Developed, Open Space <20% Impervious Surface	49	69	79	84
Developed, Low Intensity 20-49% Impervious Surface	77	86	91	94
Developed, Medium Intensity 50-79% Impervious Surface	89	92	94	95
Developed, High Intensity 80-100% Impervious Surface	98	98	98	98
Barren Land	77	86	91	94
Deciduous Forest	32	48	57	63
Evergreen Forest	39	58	73	80
Mixed Forest	46	60	68	74
Shrub	49	68	79	84
Grassland	64	71	81	89
Pasture/Hay	49	69	79	84
Cultivated Crops	71	80	87	90
Woody Wetlands	88	89	90	91
Herbaceous Wetlands	89	90	91	92

Appendix B

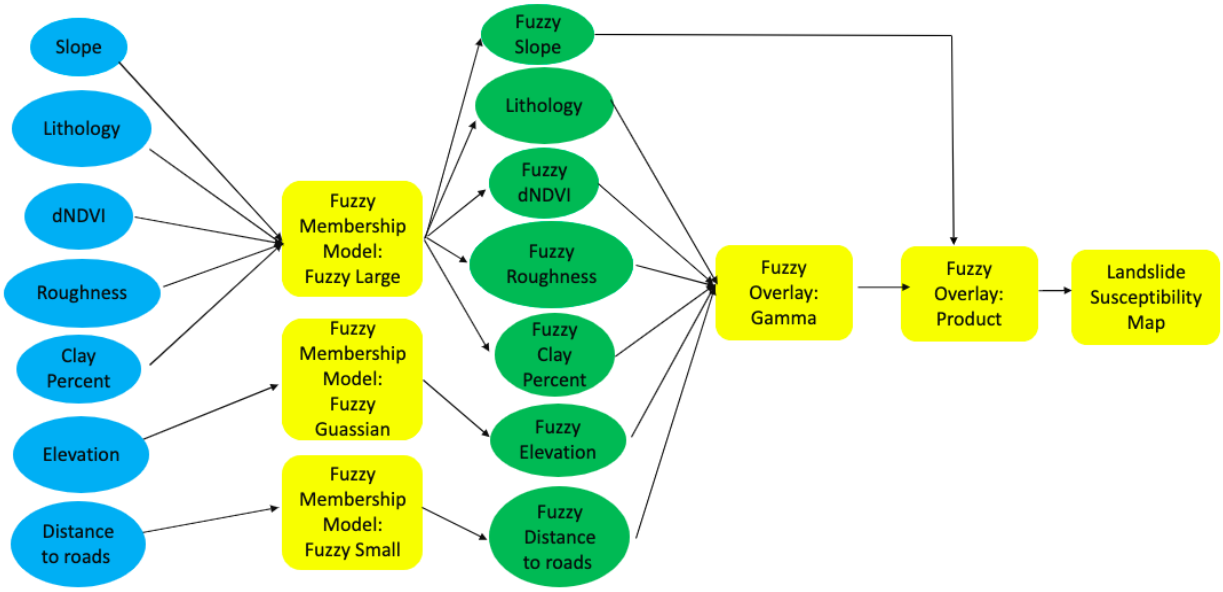

Figure B1. This flow chart depicts the process for creating a landslide susceptibility map using the Fuzzy Membership Model and Fuzzy Overlay tools in ArcGIS Pro. Fuzzy Membership reclassified the variable datasets while Fuzzy Overlay combined them. The resulting map contained the information of each factor displayed using a 0 to 1 scale with values closer to 1 representing a higher contribution to landslide susceptibility. Six out of the seven factors were combined using Fuzzy Overlay Gamma, which prevented extreme values from being favored, while slope was overlayed using the Fuzzy Overlay Product tool, this was due to slope being identified as more influential on landslide susceptibility.

Table B1

Landslide susceptibility factors displayed with the Fuzzy Membership Model type and midpoint used in the reclassification process. The Fuzzy Large type was used to place importance on larger values, such as areas with higher slopes. The Fuzzy Gaussian type uses the midpoint to define an "ideal" value which then places importance on values that are closer to the midpoint. The Fuzzy Small type focuses on smaller values.

Variable	Fuzzy Membership Type	Midpoint
Slope	Large	6.5 (unitless)
Elevation	Gaussian	200 m
Roughness	Large	3 (unitless)
Lithology	Large	1.6 (unitless)
Clay Percent	Large	27 %
dNDVI	Large	.057 (unitless)
Distance from Roads	Small	400 m

Appendix C

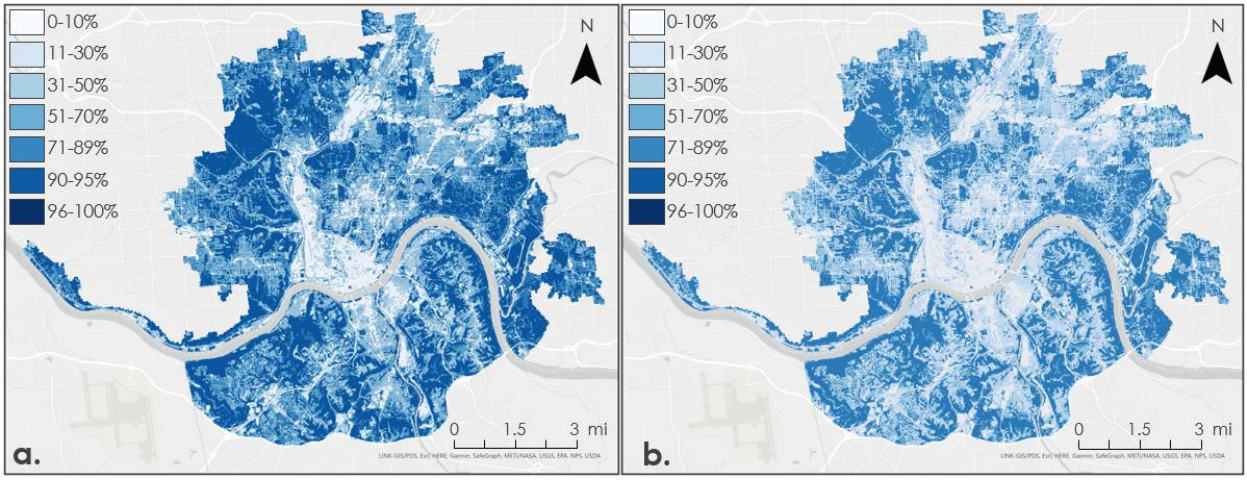

Figure C1. Runoff retention map outputs from the InVEST Urban Flood Risk Mitigation Model displaying (a) runoff retention for a 2.3-inch storm event and (b) runoff retention for a 6-inch storm event. Total percent value is representative of each rainfall event. The light blue shades indicate little to no retention while the darker blues shades gradually increase on the scale to reflect complete retention.

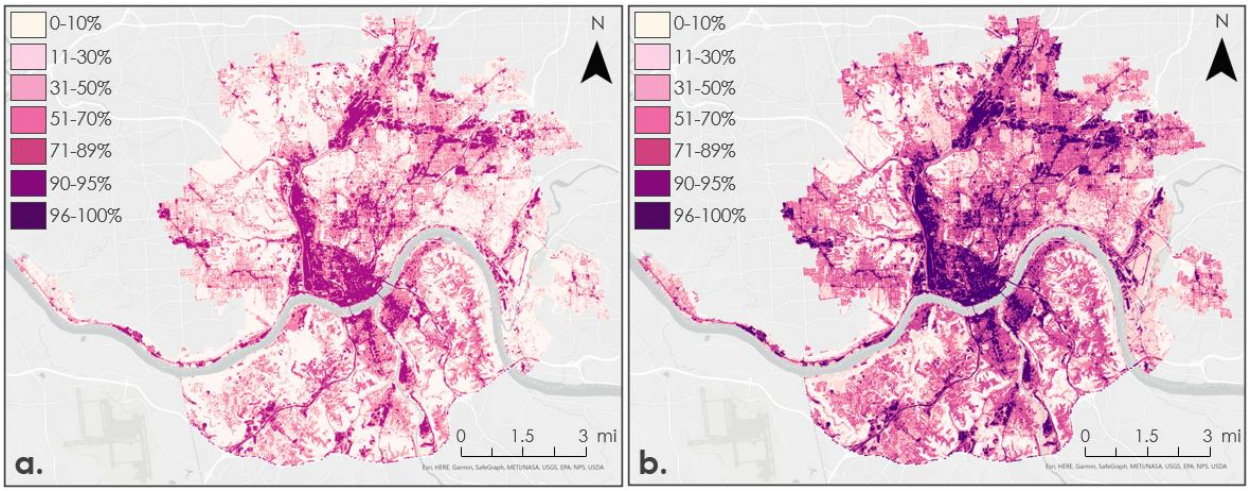

Figure C2. Runoff map outputs from the InVEST Urban Flood Risk Mitigation Model displaying (a) runoff values for a 2.3-inch storm event and (b) runoff values for a 6-inch storm event. Total percent value is representative of each rainfall event. The light pink shades indicate little to no runoff while the darker pink shades gradually increase on the scale to reflect the amount of runoff.

Appendix D

Table D1

Resulting runoff retention values and runoff values from the 60-mm (2.3 inch) and 150-mm (6-inch) daily rainfall events per LULC class produced by the InVEST Urban Flood Risk Mitigation Model.

LULC	Runoff Retention Values (inches)		Runoff Values (inches)	
	2.3-inch Rainfall Event	6-inch Rainfall Event	2.3-inch Rainfall Event	6-inch Rainfall Event
Open Water	0	0	2.3	6.0
Developed, Open Space <20% Impervious Surface	1.6	2.8	0.5	2.8
Developed, Low Intensity 20-49% Impervious Surface	0.9	1.3	1.3	4.4
Developed, Medium Intensity 50-79% Impervious Surface	0.7	0.8	1.6	5.0
Developed, High Intensity 80-100% Impervious Surface	0.2	0.2	2.1	5.6
Barren Land	0.9	1.3	1.3	4.4
Deciduous Forest	2.0	4.2	0.1	1.2
Evergreen Forest	1.8	3.3	0.3	2.2
Mixed Forest	1.9	3.4	0.2	2.1
Shrub	1.6	2.8	0.5	2.8
Grassland	1.5	2.3	0.7	3.3
Pasture	1.6	2.8	0.5	2.8
Cultivated Crops	1.6	2.4	0.6	3.2
Woody Wetlands	0.9	1.1	1.3	4.6
Herbaceous Wetlands	0.8	1.0	1.4	4.8

Appendix E

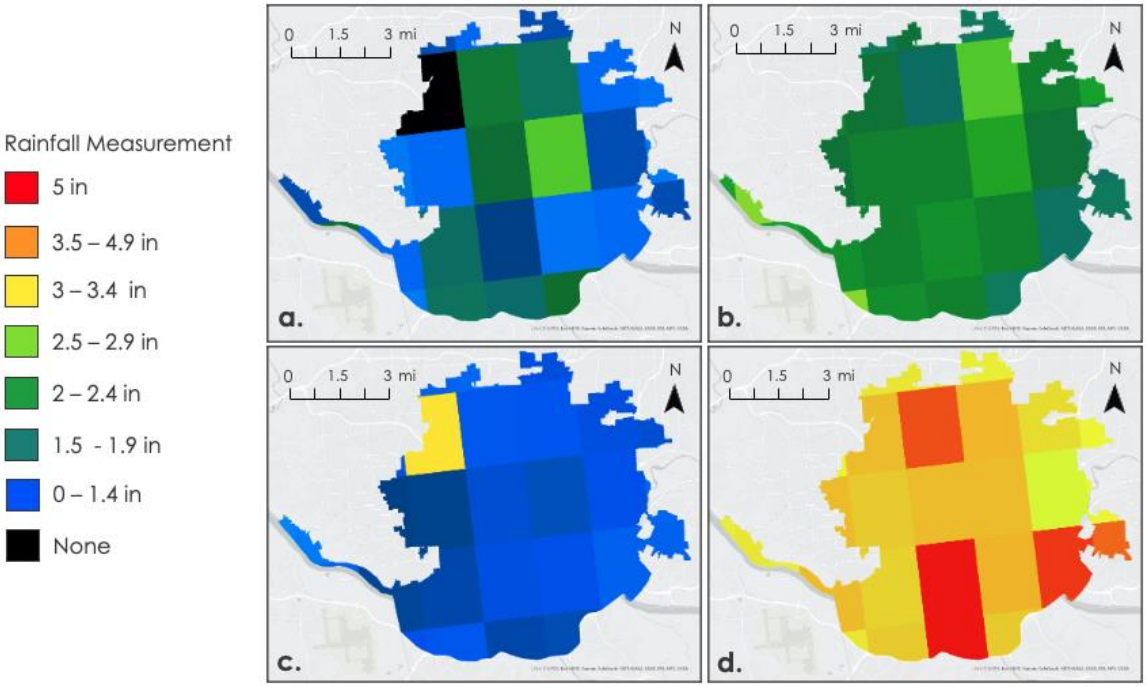

Figure E1. This plot shows rainfall variability from the CHIRPS satellite with different storm sizes shown in inches per day. The following maps display the effects of rainfall variability in millimeters from black, 0 millimeters, to red, a maximum of 128 millimeters (Figure F1). (a) A 2.3-inch recorded storm on October 10th, 2011 with a minimum of 0 inches rainfall recorded in the study area. (b) A 2.3-inch storm recorded on January 2nd , 2004 with a minimum of 1.7 inches rainfall recorded in the study area. (c) A 3.5-inch storm on October 28th, 2011 with a minimum of 0.4 inches rainfall recorded in the study area. (d) A 5-inch storm on September 26th, 2011 with a minimum of 2.9 inches rainfall recorded in the study area.

Appendix F

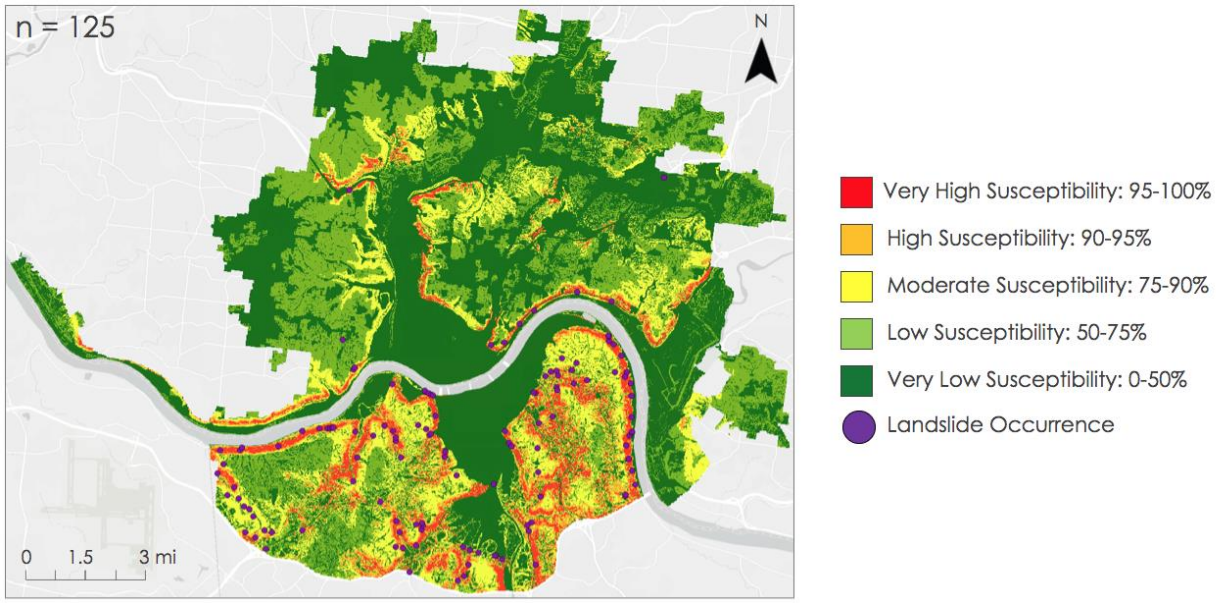

Figure F1. The landslide susceptibility map with overlaid historical inventory of 125 landslide events used for its validation. Landslide susceptibility categories correspond to five breaks in quantified risk percentile: very low (0-50th percentile, shown in dark green), low (50-75th percentile, shown in green), moderate (75-90th percentile, shown in yellow), high (90-95th percentile, shown in orange), and very high (95-100th percentile, shown in red). The spatially referenced landslide events are shown in purple.

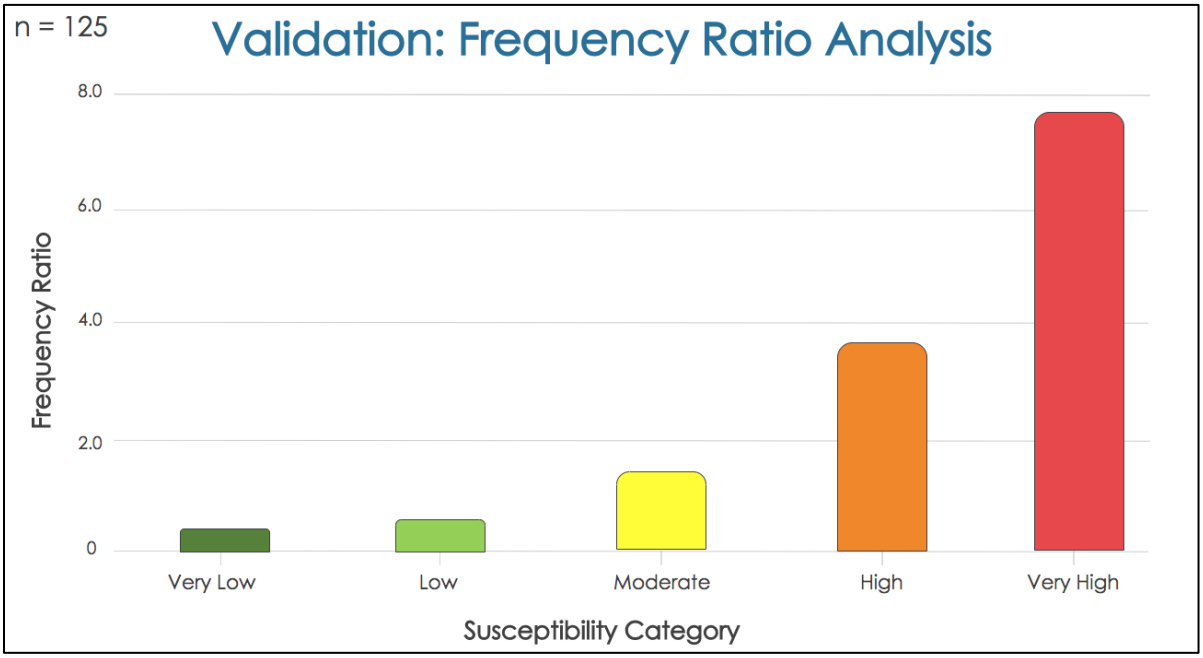

Figure F2. Plotted frequency ratios, a standardized measure of landslide occurrence, against each plotted landslide susceptibility category. Higher frequency ratios correspond to higher landslide frequency. The "Very Low" and "Low" categories on the susceptibility map capture very few landslide events, while the "Moderate," "High," and "Very High" categories cover increasingly more landslide events. These results suggest that the landslide susceptibility map is compatible with the spatial distribution of historical landslides, meaning it is accurate for the area.

Appendix G

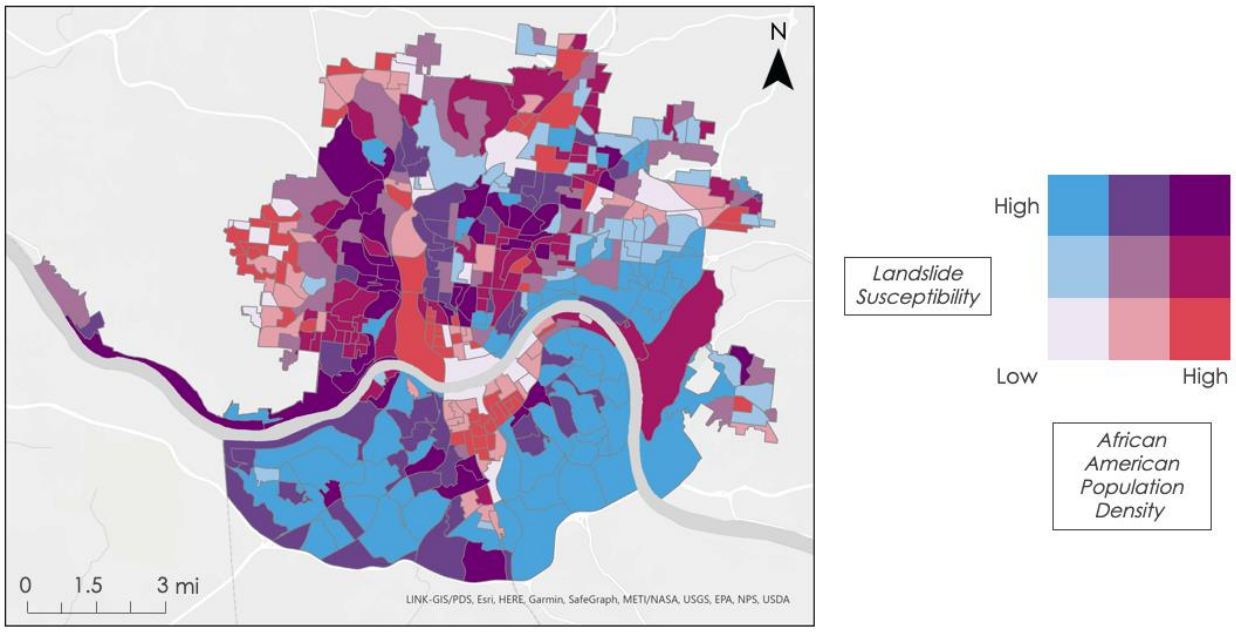

Figure G1. African American population density was displayed in relation to landslide susceptibility per census block group. Both factors were classified from High to Low before being portrayed in a bivariate color scheme method. To maintain consistency with the other exposure maps blue was used to represent landslide susceptibility, while red was chosen for African American Population density. Block groups in purple represent a combination of high susceptibility and high vulnerability.

Figure G2. 2019 impoverished population density was displayed in relation to landslide susceptibility per census block group. The population for individuals in poverty, as well as landslide susceptibility was averaged by census block groups and then classified from Low to High. A bivariate color scheme was used to highlight landslide susceptibility in blue and impoverished populations in pink, with indigo reflecting areas of high landslide exposure for individuals in poverty.

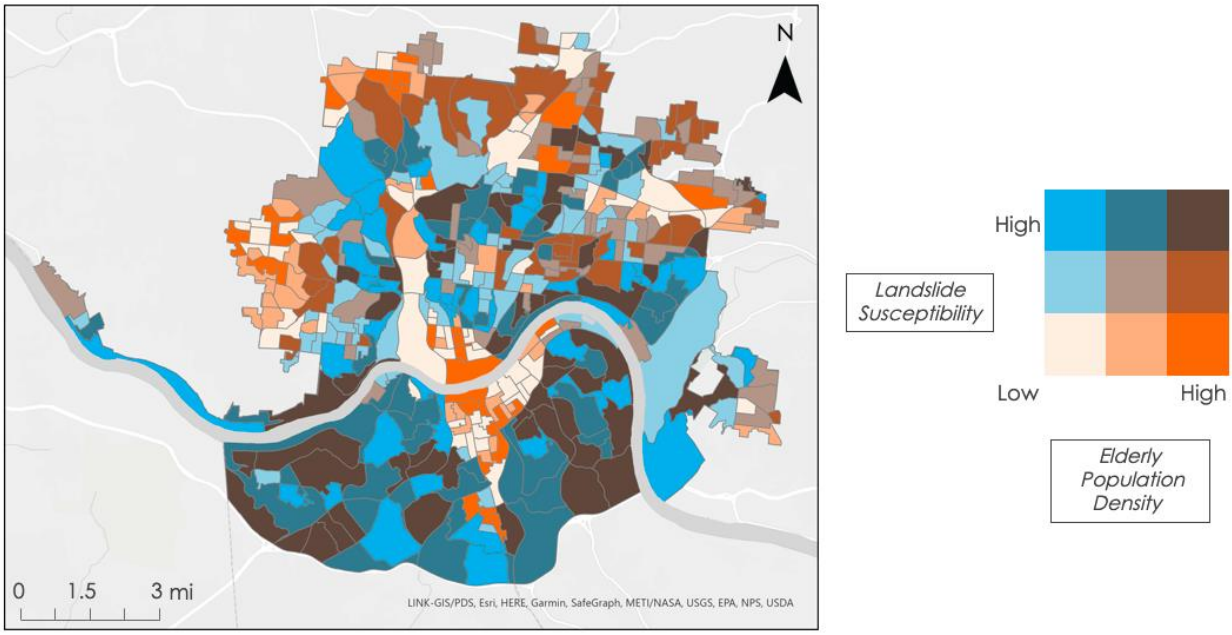

Figure G3. Elderly population, for individuals 85 years and older, was visualized in conjunction with landslide susceptibility per block group using the bivariate color scheme method. Landslide susceptibility was classified from Low to High and displayed in blue, while elderly population was also classified from Low to High then shown in orange. Brown portions of the map reflect areas of high landslide exposure for elderly populations.